

Nicholas G. Paulter Jr.,¹ John A. Ely,² and Dwight Barry³

Test Objects for the Accurate and Reproducible Evaluation of the Threat Detection Performance of Walk-Through Metal Detectors

Reference

N. G. Paulter Jr., J. A. Ely, and D. Barry, "Test Objects for the Accurate and Reproducible Evaluation of the Threat Detection Performance of Walk-Through Metal Detectors," *Journal of Testing and Evaluation* 49, no. 5 (September/October 2021): 3795–3810. <https://doi.org/10.1520/JTE20190876>

ABSTRACT

Walk-through metal detectors (WTMDs) are the mainstay for screening people for the presence of metal threat or contraband objects at security checkpoints. Although nonmetallic threats are a concern, most threats encountered in practice are metal or comprise metal components. To ensure that a WTMD will detect a given threat requires testing for that threat. However, the variety of geometries and construction of metal threats that a WTMD is expected to detect is immense, ranging from handguns to disposable razor blades and items constructed of ferromagnetic metals, nonferromagnetic metals, or both. It is unrealistic to test for all of these potential threat items. Instead, the WTMD is tested using test objects that represent classes of threats. These representative test objects must be designed so that the operator of the WTMD has confidence that the WTMD will detect the actual threat objects. The purpose of this paper is to examine the usefulness of currently used WTMD test objects to accurately and reproducibly provide an indication of WTMD detection performance and suggest new designs as appropriate.

Keywords

baseline performance, detectability, documentary standard, exemplars, test objects, threat objects, walk-through metal detector

Introduction

Walk-through metal detectors (WTMDs) are used at checkpoint security stations to search people for hidden metal objects. These objects may be threat items or contraband, depending on the required security implementation. WTMDs can be used to find metal objects

Manuscript received June 7, 2019; accepted for publication February 25, 2020; published online April 3, 2020. Issue published September 1, 2021.

¹ National Institute of Standards and Technology, 100 Bureau Dr., Mail Stop 8102, Gaithersburg, MD 20899, USA (Corresponding author), e-mail: nicholas.paulter@nist.gov, <https://orcid.org/0000-0002-9782-0894>

² Federal Bureau of Prisons (retired), 4795 Sherry Dr., Mount Airy, MD 21771, USA

³ National Institute of Standards and Technology, 100 Bureau Dr., Mail Stop 8102, Gaithersburg, MD 20899, USA

hidden inside body cavities or underneath skin folds, which advanced imaging technologies¹⁻³ typically cannot do. Therefore, the detection performance of WTMDs must be accurately known and reproducibly measured or assessed. Knowing the performance of a WTMD will help in product selection, deployment strategies, and modeling of multitechnology security solutions. The detection performance of a WTMD is obtained using appropriate test methods, test objects, and analysis methods. These test methods should thoroughly exercise the detection performance of the WTMD, which was the subject of Larson, Paulter, and Troje⁴ and Paulter⁵ and will not be addressed here. The effect of the test object on the assessment of WTMD baseline detection performance is examined here.

The baseline performance is the performance level below which a WTMD is deemed not adequate for security and safety applications. Having baseline performance requirements facilitates the procurement and selection process because only those WTMDs that meet these performance requirements should be considered for employment or further agency-specific assessment. The only currently published WTMD standard that contains baseline performance requirements is the outdated National Institute of Justice (NIJ) Standard 0601.02,⁶ *Walk-Through Metal Detectors for Use in Concealed Weapon and Contraband Detection*, which comprises several detection performance requirements: test object detectability (detection sensitivity), test object transit speed, detection repeatability, throughput rate, and discrimination. ASTM publishes a standard practice⁷ for assessing the detection performance of WTMDs that includes test object design.

We have previously identified the test methods that will provide accurate and reproducible measures of threat object detectability⁵ in a WTMD. This study will examine the utility of the different test objects currently in use to provide estimates of WTMD detection performance. These test objects are either described in the NIJ standard or have been required for product evaluation by different US federal agencies. The ASTM test objects⁷ have not been used routinely for WTMD evaluation and are not considered here.

Metal detection technology is employed for other applications, such as buried landmine detection⁸⁻¹⁰ and unexploded ordnance (UXO) detection.¹¹⁻¹⁵ Often, in these cases, inductance spectroscopy or other inductive methods are used to gain more information on the possible threat because of the ubiquity of clutter.

Previous studies on WTMD testing have been reported,^{16,17} but the design of the test objects was not comparatively addressed, whereas this study is focused on comparing the efficacy of the test objects for quantifying WTMD detection performance. This study does not address designs that exploit the magnetic polarizability tensor,^{18,19} as these designs are not commercially available or fielded.

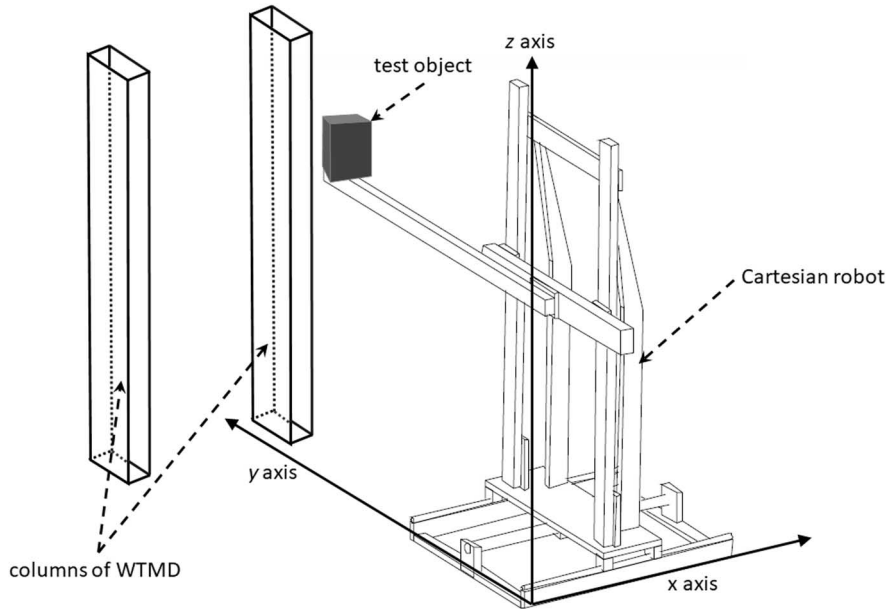
This study examines the detectability of test objects of the size classes of large, medium, and small, nominally as defined in NIJ Standard 0601.02,⁶ for both ferromagnetic and nonferromagnetic test objects. These results have applications in procurement requirements as well as documentary performance standards, similar to the ASTM standards for hand-worn metal detectors²⁰ and handheld metal detectors,²¹ both of which were driven by similar studies for hand-worn and handheld metal detectors.^{22,23}

The test objects are used to assess the detection performance of a WTMD using a measure of the probability of detection, p_d , and probability of false alarm, p_{fa} . To facilitate the assessment of WTMD detection performance, test objects are segregated into different categories, such as object size, which is adopted here. The p_d for the least-detectable test object for a given size class should establish the baseline detection performance of the WTMD. Using the least-detectable test objects for the baseline will ensure that all threat items larger than the least-detectable test object will be detected for that size class. This least-detectable test object will represent a given class of threat objects, such as handguns, knives, or other threat items. The size segregation also facilitates defining innocuous items, which are items that should not cause an alarm in certain situations, wherein these alarms (also called nuisance alarms) may cause lengthy delays in security screening. For example, in certain situations, the security protocol is to prevent handgun entry but not to stop knives or other objects from entry.

Test Methods

The National Institute of Standards and Technology (NIST) metal detector measurement system was used to perform this study²⁴ (see [fig. 1](#)). This system comprises a cartesian robot that pushes a test object through

FIG. 1 Sketch of the measurement system showing the Cartesian robot and two columns of a WTMD.



the WTMD portal at fixed entry-point locations at specified velocities following a rectilinear trajectory. This trajectory is parallel to the axis running through the portal of the WTMD (labeled as the y axis). The entry-point locations are defined in the x - z plane of the WTMD, where the z axis is parallel to the vertical direction and the x axis is normal to the z axis and to the y axis.

The test methods research performed in Paulter⁵ demonstrated that the detectability of a test object as a function of the test object entry-point location in the WTMD portal, test object orientation, scan speed, and scan trajectory (rectilinear and nonrectilinear) was nominally the same for different WTMD models and different WTMD detection-sensitivity-related settings. Consequently, one WTMD model was selected for this study. Based on the results of Paulter⁵ and the fact that the data acquisition rate is fixed and does not change with scan speed, a scan speed of 0.2 m/s was selected, as this provides four usable samples for each scan and does not affect test object detectability. A usable sample is one that is taken from about the central half of the scan data. The entry-point locations for the scans are described by a 27-position (3 horizontal by 9 vertical) array. The horizontal positions referenced from the inner surface of one side of the WTMD portal are approximately 150, 300, and 450 mm for a portal width of nominally 600 mm. The vertical locations are approximately 100; 300; 500; 700; 900; 1,100; 1,300; 1,500; and 1,700 mm.

The test objects used in this study are those that are frequently used for verification of the performance of WTMDs. These objects include the ones described in the National Institute of Law Enforcement and Criminal Justice (NILECJ) Standard 601 and the NIJ Standard 0601.02, the North American Arms (NAA) 22-caliber revolver, and the Davis¹ 32 caliber derringer, both assembled and disassembled. (Note: Mention of a manufacturer or product in this manuscript does not imply endorsement of the manufacturer or product by NIST or the authors. The products mentioned here have been used as de facto detection artifacts for WTMD testing.)

Although the detection signal values that are caused by test objects passing through the portal of the WTMD are used here in comparing test object detectability, it should be noted that it is the generation of an alarm by the WTMD that is the basis for the security function. The WTMD provides an alarm if the object passing through the WTMD portal produces a detection signal that exceeds a threshold value, which may happen anywhere along the trajectory of the test object through the portal.

Data Analysis

The data were collected for a set of 27 unique entry-point locations in the portal. For each of these locations, 20 scans were performed. For each of these 20 scans, a maximum, minimum, and average value was obtained (see [fig. 2](#)). These values were then averaged over the 20 scans to provide 1 value for each of the 27 entry-point locations for each test object. These values are used (1) for p_d to determine the test object for each size category that provides the least detectable signature for any location in the WTMD portal and (2) for p_{fa} for each size category to determine the test object that provides the most detectable signature for any location in the WTMD portal. For (1), then, the p_d requirement should be based on the signal level corresponding to the minimum of the scan maxima for all test objects of the same size category, that is, based on the following:

$$\min_{\max_{obj}} = \min\{\max_{obj,loc}\} \quad (1)$$

where

$$\max_{obj,loc} = \frac{1}{20} \sum_{i=1}^{20} \max_{obj,loc,i} \quad (2)$$

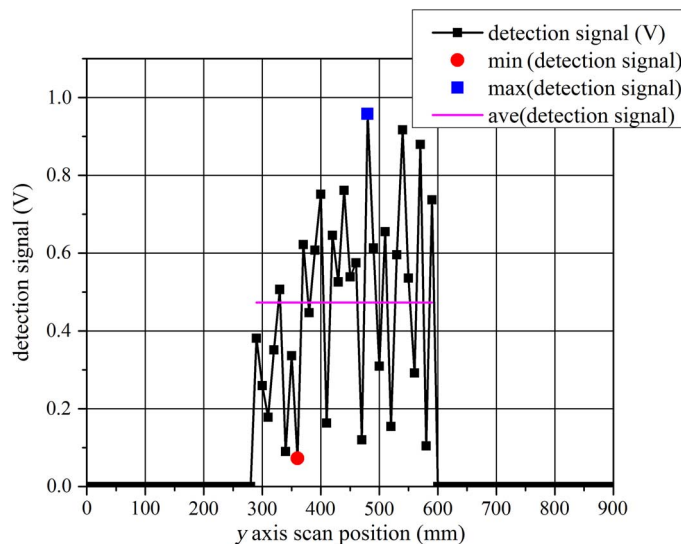
and

$$\max_{obj,loc,i} = \max\{s_{obj,loc,i}\}, \quad \text{for all } i \quad (3)$$

and $s_{obj,loc,i}$ is the real-valued detection signal (a four-element sequence as described in the “Test Methods” section) output by the WTMD for a given object (indicated by subscript “ obj ”), for a given entry-point location (indicated by the subscript “ loc ”), and for a given scan (indicated by the index “ i ”); $\max\{\}$ returns the maximum value of its argument, and $\min\{\}$ returns the minimum value of its argument. The $\min_{\max_{obj}}$ is the signal level for each test object that occurs at the entry-point location that causes that test object to be the least detectable. For each possible text object, there is a $\min_{\max_{obj}}$. We compare the sets of $\min_{\max_{obj}}$ for each size class and material class (ferromagnetic and nonferromagnetic) to identify that test object with the least value

FIG. 2

Example of data from a scan of an entry-point location in the portal of the WTMD. The scan starts and stops outside the portal region of the WTMD; therefore, the average and minimum detection values for the scan are computed only using the part of the scan that is within the portal.



for $min_{max_{obj}}$ in that class. The rationale for selecting the least of $min_{max_{obj}}$ is that the least-detectable test object of a given size class should set the threshold for detection, and this should reduce the probability that smaller items will cause an alarm. The results presented here are $min_{max_{obj}}$ and standard uncertainty for the 20 scans. For (2), the p_{fa} requirement should be based on the signal level corresponding to the maximum of the scan maxima for all innocuous items of the same size category, which is based on the following:

$$max_{max_{obj}} = \max\{max_{obj,loc}\} \tag{4}$$

For illustrative purposes, plots of the $max_{obj,loc}$, $min_{obj,loc}$, and $ave_{obj,loc}$ for the test object NILECJ AM9 for its minimum detectability orientation are shown in **figure 3**, which show the variability of the test object detectability across the portal of the WTMD for different attributes of the signal (maximum value, average value, and minimum value). **Figure 4** shows the relative difference in detectability for different test objects through $ave_{obj,loc}$ for the NAA 22-caliber revolver assembled, the NAA 22-caliber revolver disassembled (that is, without the cylinder), and the NIJ 0601.02 steel handgun exemplar.

Results

Results of measurements on different test objects are presented in this section.

LARGE FERROMAGNETIC TEST OBJECTS

The large ferromagnetic test objects that are considered include the NILECJ AM9, the NILECJ AM7, the NILECJ AM5, the NILECJ AM3, the fully assembled (commonly referred to as “assembled”) NAA 22-caliber revolver, the NAA 22-caliber revolver missing the cylinder (commonly referred to as “disassembled”), and the NIJ Standard 0601.02 steel handgun exemplar (see **Table 1**). The results for the $min_{max_{obj}}$ values for these test objects are shown in **Table 1**. For the large ferromagnetic test object, the test object that provided the least detectability is the NIJ 0601.02 steel handgun exemplar.

FIG. 3 Detectability scan maps for test object NILECJ AM9 at its orientation giving minimum detectability. The leftmost plot displays the maximum value of the 20 scans, the middle plot the average value of the 20 scans, and the rightmost plot the minimum value for the 20 scans. The measurement uncertainty for each datum shown in the plots ranged from about 5 % of datum value to about 20 %.

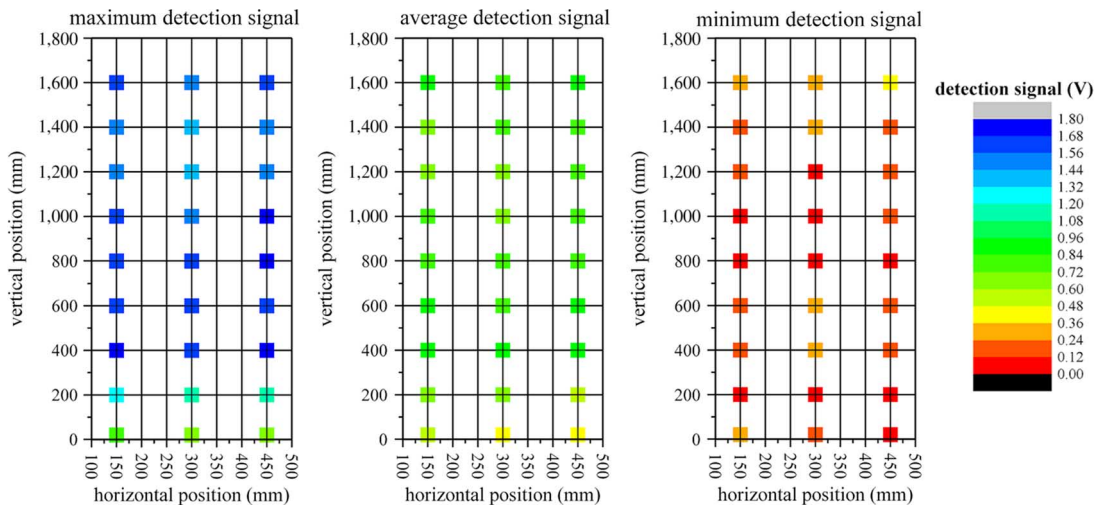


FIG. 4 Detectability scan maps for the indicated test objects at their orientation giving minimum detectability. The plots display the average value of the 20 scans. The measurement uncertainty for each datum shown in the plots ranged from about 5 % of datum value to about 20 %. The leftmost plot shows the scan map for the assembled-NA-22 test item, the middle plot for the disassembled-NA-22 test item, and the rightmost plot for the NIJ0601.02 steel-handgun test item.

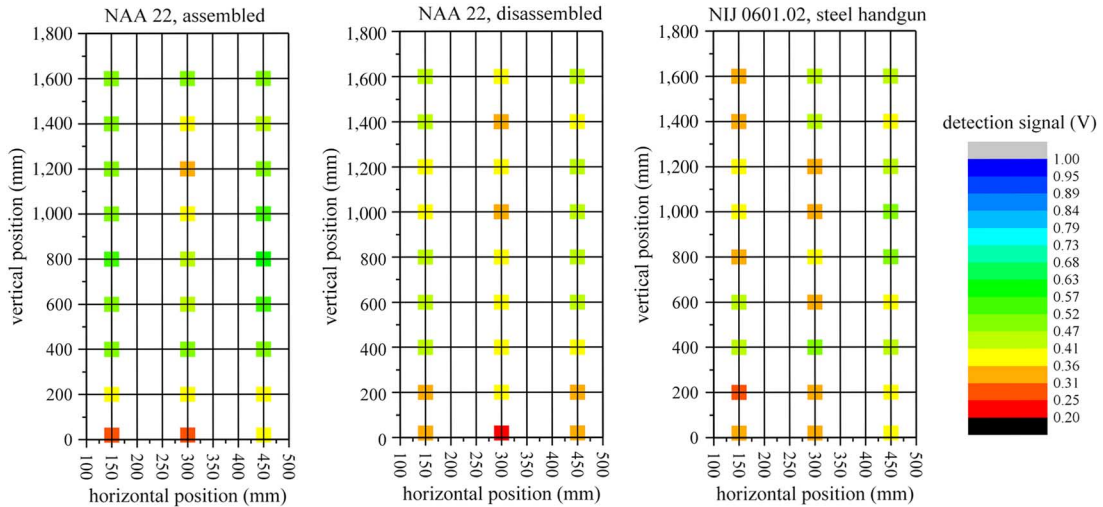


TABLE 1
 $min_{max,obj}$ values for the large ferromagnetic test objects

Size and Material Category	Test Object	$min_{max,obj} \pm V$
Large, ferromagnetic	NILECJ AM9	0.623 ± 0.047
	NILECJ AM7	0.607 ± 0.040
	NILECJ AM5	0.629 ± 0.036
	NILECJ AM3	0.563 ± 0.052
	NAA 22, assembled	0.700 ± 0.009
	NAA 22, disassembled	0.537 ± 0.025
	NIJ 0601.02 steel handgun	0.502 ± 0.023
Large, nonferromagnetic	NILECJ AN7	0.615 ± 0.008
	NILECJ AN5	0.524 ± 0.042
	Davis 32, assembled	0.490 ± 0.008
	NIJ 0601.02 zinc handgun	0.517 ± 0.007
Medium, ferromagnetic	NILECJ AM1	0.129 ± 0.004
	NILECJ B5	0.337 ± 0.007
	NIJ 0601.02 steel knife	0.149 ± 0.016
Medium, nonferromagnetic	NILECJ AN1	0.128 ± 0.007
	NILECJ AN3	0.255 ± 0.001
	NIJ 0601.02 aluminum knife	0.127 ± 0.010
	Davis 32, disassembled	0.216 ± 0.002
Small, ferromagnetic	NILECJ B2	0.105 ± 0.003
	NIJ 0601.02 #2 Phillips screwdriver bit	0.073 ± 0.016
Small, nonferromagnetic	NIJ 0601.02 22-caliber bullet	0.041 ± 0.016
	NIJ 0601.02 nonferromagnetic stainless steel knife	0.068 ± 0.023
	Stainless steel rod, 6-mm diameter, 80-mm long	0.005 ± 0.014

LARGE NONFERROMAGNETIC TEST OBJECTS

The large nonferromagnetic test objects that are examined include the NILECJ AN7, the NILECJ AN5, the Davis 32 caliber derringer assembled, and the NIJ Standard 0601.02 zinc handgun exemplar (see [Table 1](#)). The barrels in the Davis 32 derringer are ferromagnetic. The results for the $min_{max_{obj}}$ values for these test objects are shown in [Table 1](#). For the large nonferromagnetic test object, the test object that is the least detectable is the Davis 32 caliber derringer assembled. The NIJ 0601.02 zinc handgun exemplar has a $min_{max_{obj}}$ very close to that of the assembled Davis 32 handgun and, with a modification in size, could be used to replace the assembled Davis 32 handgun. This is discussed in the “ p_d Test Objects” section. The purpose of using a modified NIJ 0601.02 zinc handgun exemplar instead of the Davis 32 handgun is reproducibility of manufacture and consistency over time.

MEDIUM FERROMAGNETIC TEST OBJECTS

The medium ferromagnetic test objects that are examined include the NILECJ AM1, the NILECJ B5, and the NIJ Standard 0601.02 steel knife exemplar, and results for the $min_{max_{obj}}$ values for these test objects are shown in [Table 1](#). For the medium ferromagnetic test object, the least-detectable test object is the NILECJ AM1. The NIJ 0601.02 steel knife exemplar has a $min_{max_{obj}}$ very close to that of the NILECJ AM1 and, with a modification in size, could be used to replace the NILECJ AM1. This is discussed in the “ p_d Test Objects” section. The NILECJ AM1 is a solid cylinder, and the purpose for a modification to the NIJ 0601.02 steel knife exemplar would be to create a test object that is similar in appearance to a knife. Similarities to actual threat objects are preferred by both the user community and manufacturers for establishing baseline performance standards and procurement documents.

MEDIUM NONFERROMAGNETIC TEST OBJECTS

The medium nonferromagnetic test objects that are considered include the NILECJ AN1, the NILECJ AN3, the Davis 32 caliber derringer disassembled (missing the barrels), and the NIJ Standard 0601.02 aluminum knife exemplar results for the $min_{max_{obj}}$ values for these test objects are shown in [Table 1](#). The disassembled Davis 32 is included in this class as it has a detection signal similar in magnitude to other objects in this class. For the medium nonferromagnetic test object, the least-detectable test object is the NIJ 0601.02 aluminum knife exemplar. Although the NILECJ AN1 has a very similar $min_{max_{obj}}$ compared with the aluminum-knife exemplar, the latter is selected for similarity to the actual threat.

SMALL FERROMAGNETIC TEST OBJECTS

The small ferromagnetic test objects examined include the NILECJ B2 and the NIJ Standard 0601.02 #2 Phillips screwdriver bit exemplar (see [Table 1](#)). A previous study demonstrated that the NIJ Standard 0601.02 #2 Phillips screwdriver bit exemplar was the least detectable of the NIJ Standard 0601.02 small ferromagnetic test objects.²⁰ The $min_{max_{obj}}$ values for these test objects in their least detectable orientation are given in [Table 1](#). The least-detectable test object for this category is the #2 Phillips screwdriver bit exemplar in its minimum detection orientation. The minimum detection orientation is where the long axis of the screwdriver bit exemplar is parallel to the height (vertical axis) of the WTMD.

SMALL NONFERROMAGNETIC TEST OBJECTS

The small nonferromagnetic test objects examined include the NIJ Standard 0601.02 22-caliber bullet exemplar, the NIJ Standard 0601.02 nonferromagnetic stainless steel knife exemplar, and a nonferromagnetic stainless steel rod that has been broadly accepted as an example of a hard-to-detect object, and $min_{max_{obj}}$ values for these test objects in their least-detectable orientation are given in [Table 1](#). The least-detectable test object for this category is the stainless steel rod with its length aligned to be parallel to the width of the WTMD. However, this test object may not be detectable by most WTMDs and should not be used in a baseline performance standard. The NIJ 0601.02 22-caliber bullet exemplar with its long axis parallel to the width (horizontal axis) of the WTMD portal should be used as the small nonferromagnetic test object.

TEST OBJECTS FOR p_{fa}

The innocuous test items require selection considerations similar to that for the p_d test objects. The consideration for the innocuous test item is that maximumly detectable innocuous item should be less detectable than the test object of the associated size category. In this case, if the test object is not detected, then the innocuous item is not likely to be detected. The innocuous item test objects, historically, have not been grouped according to material properties and so will not be here. There are two size classes for the innocuous items, large and medium. The $max_{max_{obj}}$ values for the four innocuous test objects are given in [Table 2](#).

Innocuous Items for Large-Size Class

Any of the innocuous items given in [Table 2](#) could be used for a large-object innocuous test object because the $max_{max_{obj}}$ of the innocuous test objects is less than the $min_{max_{obj}}$ of the large-size test objects. To facilitate baseline performance measurements and minimize confusion regarding which WTMD regions to use for the different innocuous test objects, the use of one innocuous test object throughout the volume of the WTMD portal would be preferred. One innocuous test object would also facilitate WTMD model comparison. Suggestions for alternate large-size innocuous test object designs will be discussed in the “ p_{fa} (Innocuous) Test Objects” section.

Innocuous Items for Medium-Size Class

It can be seen by comparing $max_{max_{obj}}$ from [Table 2](#) with $min_{max_{obj}}$ from [Table 1](#) that only the NIJ 0601.02 belt buckle exemplar could act as a possible innocuous item for the medium-size category if it is limited to a partial vertical range. Requiring different innocuous test objects for different regions of the WTMD portal would introduce additional measurement complexity that is not necessary. The innocuous test object should be able to be used over the entire volume of the WTMD portal. Alternate designs for the medium-size innocuous test object will be discussed in the “ p_{fa} (Innocuous) Test Objects” section.

EFFECT OF TEST OBJECT ROTATION ON DETECTABILITY

The test object orientation has been previously demonstrated to affect test object detectability.⁴ These orientations describe the alignment of the major axes of the test object with the vertical axis, Z_{WTMD} , of the WTMD and with the faces of the test object perpendicular to the direction of propagation (see [fig. 5](#)).

The rotations considered here are around the major axes of the WTMD: X_{WTMD} , Y_{WTMD} , and Z_{WTMD} , where X_{WTMD} is the direction between the left and right panels of the WTMD, Y_{WTMD} is the direction of travel through the WTMD, and Z_{WTMD} is along the vertical direction in the WTMD. To measure the effect of rotation on test object detectability, the NIJ 0601.02 steel knife exemplar is used. This exemplar has nine unique sets of starting faces and rotation axes for the rotation measurements (see [Table 3](#) and [fig. 6](#)).

TABLE 2
 $max_{max_{obj}}$ values for the innocuous test objects over different vertical ranges of the WTMD

Test Object	$max_{max_{obj}}, V$
NIJ 0601.02 belt buckle	...
• 600 to 1,000 mm	0.075 ± 0.026
• Full range	0.133 ± 0.010
NIJ 0601.02 eyeglasses	...
• 1,200 to 1,600 mm	0.305 ± 0.004
• Full range	0.318 ± 0.006
NIJ 0601.02 set of coins	...
• 600 to 1,000 mm	0.311 ± 0.005
• Full range	0.311 ± 0.005
NIJ 0601.02 watch	...
• 400 to 800 mm	0.330 ± 0.010
• Full range	0.330 ± 0.010

FIG. 5 Orientations of knife exemplar relative to vertical axis, Z_{WTMD} , of the WTMD. The numbered arrows indicate the direction of travel of the exemplar through the WTMD portal, and these are used for orientation numbering.⁴ The unique faces of the exemplar are indicated by F1, F2, and F3. The red arrows indicate the major axes of the exemplar.

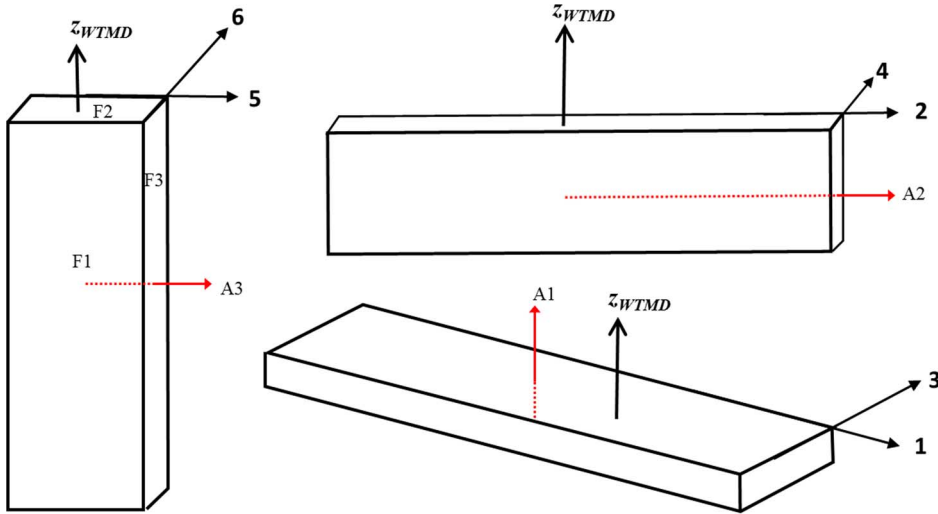


TABLE 3

Rotation measurement axes for steel knife exemplar; see figure 5. The face designation in the leftmost column indicates the face of the exemplar (see top sketch in fig. 6) that is perpendicular to the indicated rotation axis, which is one of the axes of the WTMD portal (see bottom sketch in fig. 6)

Face Perpendicular to Rotation Axis	Rotation Axis
F1	X_{WTMD}
	Y_{WTMD}
	Z_{WTMD}
F2	X_{WTMD}
	Y_{WTMD}
	Z_{WTMD}
F3	X_{WTMD}
	Y_{WTMD}
	Z_{WTMD}

In figure 7, the change in the detection signal relative to the rotation giving the least detection signal is shown. This change is computed using the following:

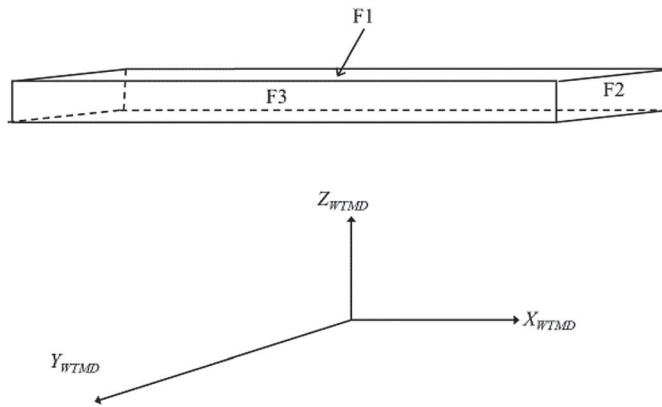
$$\Delta ave_{max} = \left(1 - \frac{\text{least}(ave_{max,obj})_{ep1}}{\text{greatest}(ave_{max,obj})_{ep1}} \right) 100\% \tag{5}$$

where $\text{least}(x)_{ep1}$ gives the least value of x for all the tested entry-point locations, and $\text{greatest}(x)_{ep1}$ gives the greatest value of x for all the tested entry-point locations, and

$$ave_{max,obj} = \frac{1}{27} \sum_{loc=1}^{27} max_{obj,loc} \tag{6}$$

FIG. 6

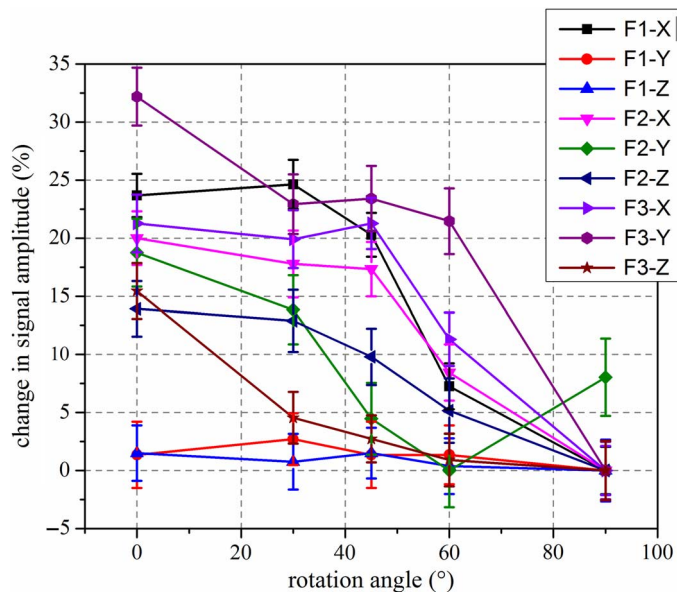
The unique faces of the steel knife exemplar and the axes of rotation.



From **figure 7**, it can be seen that the effect of rotation for a given starting configuration depends on that configuration. In some cases, F1-Y and F1-Z for example, the effects of rotations are within measurement uncertainty (indicated by the bars in **fig. 7**). Most configurations do show an effect of rotation. The worst case is about a 30 % effect. Depending on the threshold level setting to generate an alarm, the rotation effect may incorrectly cause the WTMD to alarm on a test object that is expected to be in its least-detectable orientation when, in fact, it is not. The rotation effect is not as pronounced as was observed for handheld and hand-worn metal detectors,²³ and this is due to the complex magnetic field within the WTMD portal volume that is the result of several transmit coils, where each transmit coil may have a different geometry and may overlap with adjacent coils. In comparison, the handheld and hand-worn metal detectors typically employ one coil. Because of the effect of test object rotation on test object detectability, the rotation of the test object should be controlled during testing. However, because of the many contributors to the rotational uncertainty of the test object relative to the metal detector, it may be difficult to accurately control this rotation and to

FIG. 7

Rotations about different faces of the NIJ 0601.02 steel handgun exemplar. The face references are given in **figure 5**. The axes of rotation are indicated by “X,” “Y,” and “Z.” As an example, “F1-Y” means that face F1 is rotated about the y axis. The vertical bars indicate the approximate 65 % (one sigma) measurement uncertainty.



reproducibly and accurately assess the technical detection performance of a WTMD. Test objects that would not be subject to rotation and orientation effects are discussed in the “Spherical Test Objects” section.

Alternate Test Object Design

The purpose of this section is to explore different designs for the test objects. The first part of this section will consider traditional test object designs, that is, designs that nominally have an appearance similar to the threat but are simple to manufacture and are manufactured using materials of known characteristics, such as composition (via Unified Numbering System (UNS) designations), magnetic permeability, and electrical conductivity. The material requirements ensure reproducibility of the test object detectability.

ρ_d TEST OBJECTS

Two test objects were suggested for replacement in previous sections (“Large Nonferromagnetic Test Objects” and “Medium Ferromagnetic Test Objects”): the Davis 32 caliber derringer assembled to be replaced by a modified version of the NIJ 0601.02 zinc handgun exemplar and the NILECJ AM1 to be replaced by a modified version of the NIJ 0601.02 steel knife exemplar. Both modifications were performed by reducing the size of the NIJ test objects. The results are shown in **Tables 4** and **5**, whereas the orientations and geometries are shown in **figures 5**, **6**, and **8**. These tables show the dimensions of a reproducible test object that can be used for the large nonferromagnetic test object and the medium ferromagnetic test object. For the NIJ 0601.02 steel knife exemplar, these test locations were for the smallest z -axis values (that is, closest to the floor); see **figure 9**. Although the detectability of a test object is dependent on entry-point location, it can be seen in **figure 9** that the nominally 65 by 15 by 1.6-mm steel knife exemplar is the least detectable of the group for all entry-point locations. Note that the ideal goal is to have the modified steel knife exemplar be the least-detectable test object for all entry-point locations tested. However, because of day-to-day variations in WTMD response (repeatability), it will likely be difficult to ensure that the selected test objects will always provide a smaller detection signal than the threat object. Moreover, as the purpose is to develop test objects that describe the baseline performance of the WTMD, the ideal goal of the test object being less detectable than the threat object for all entry-point locations is not necessary, as the end user should test the WTMD for their specific threats.

FIG. 8
Sketch of NIJ 0601.02 zinc handgun exemplar.

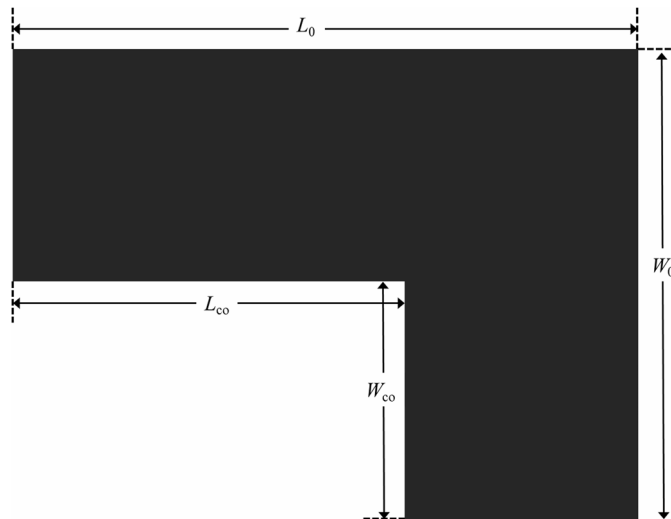


TABLE 4

$min_{max_{obj}}$ values for the modified test objects. The NIJ 0601.02 zinc handgun exemplar is an “L”-shaped extrusion (see **fig. 8**) of zinc (UNS Z35530) with a thickness of $14.257 \text{ mm} \pm 0.1 \text{ mm}$. The overall length, L_0 , and the overall width, W_0 , of the exemplar and the width, W_{co} , and length, L_{co} , of the cutout to make an “L”-shaped extrusion are given

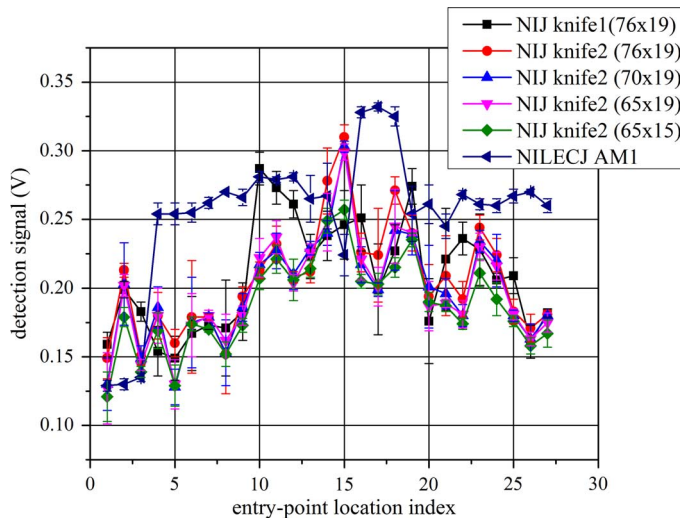
Test Object	Size, mm				$min_{max_{obj}}, V$
Davis 32, assembled	As Manufactured				0.415 ± 0.015
NIJ 0601.02 zinc handgun	L_0	W_0	L_{co}	W_{co}	...
Mod0 (no modification)	76 ± 0.1	57 ± 0.1	48 ± 0.1	29 ± 0.1	0.416 ± 0.003
Mod1	76 ± 0.1	57 ± 0.1	48 ± 0.1	37 ± 0.1	0.378 ± 0.067
Mod2	76 ± 0.1	57 ± 0.1	56 ± 0.1	37 ± 0.1	0.351 ± 0.049

TABLE 5

$min_{max_{obj}}$ values for the modified test objects. The NIJ 0601.02 steel knife exemplar is a parallelepiped of steel (UNS G41300) with a thickness of $1.6 \pm 0.1 \text{ mm}$. The length, L , and width, W , of the exemplar are given. Two samples, given by “knife1” and “knife2,” were tested to verify the reproducibility of test object response. Tests on the modified steel knife exemplar were based on Sample #2

Test Object	Size, mm		$min_{max_{obj}}, V$
NILECJ AM1	As Manufactured		0.129 ± 0.004
NIJ 0601.02 steel knife	L	W	...
knife1	76 ± 0.1	19 ± 0.1	0.149 ± 0.016
knife2	76 ± 0.1	19 ± 0.1	0.149 ± 0.015
knife2	70 ± 0.1	19 ± 0.1	0.128 ± 0.013
knife2	65 ± 0.1	19 ± 0.1	0.127 ± 0.026
knife2	65 ± 0.1	15 ± 0.1	0.121 ± 0.018

FIG. 9 The $max_{obj,loc}$ for the different test objects as a function of the entry-point location. There were 27 entry-point locations: 3 columns and 9 rows. The bottom row of the scan corresponds to entry-point location indexes of 1, 2, and 3 and is located nearest to the WTMD floor. “Knife1” and “knife2” are two distinct test pieces. The values in parentheses show the length and width of the text object in millimeters.



For the NIJ 0601.02 zinc handgun exemplar, the width of the barrel and the handle of exemplar were reduced from approximately 28 mm to approximately 20 mm. These reductions resulted in a test object with a similar detectability to that of the assembled Davis 32. For the NIJ-0601.02-steel knife exemplar, the length and width were both reduced to obtain signal levels nominally equivalent to those of the NILECJ AM1 obtained nearest the WTMD floor.

p_{fa} (INNOCUOUS) TEST OBJECTS

The recommendation in the “Test Objects for p_{fa} ” section for the alternative innocuous test object design is to use the next smaller size class for discrimination. That is, for a WTMD to alarm on large-size threat objects, the innocuous item should be a medium-size test object. Specifically, it should be the medium-size test object that provides the greatest value of $max_{max_{obj}}$, but the WTMD should be set to alarm at $min_{max_{obj}}$ of the selected large test object. For the large ferromagnetic class, the selected test object is the NIJ 0601.02 steel handgun exemplar, which has a $min_{max_{obj}}$ of 0.502 ± 0.023 V. Of the medium ferromagnetic test objects examined, the NILECJ AM1 would be suitable with a $max_{max_{obj}}$ of 0.332 ± 0.003 V. The NILECJ AM1 could also be used for the innocuous test object for the large nonferromagnetic class. Furthermore, by modification of the NIJ 0601.02 steel knife exemplar to replace the NILECJ AM1 as described in the “ p_d Test Objects” section, the reduced-size (65 by 15 by 1.6 mm) steel knife exemplar could be used as the large-size innocuous-item test object.

A similar argument can be presented for using the nonferromagnetic stainless steel rod with a nominal 6-mm diameter and nominal 80-mm length ($max_{max_{obj}}$ of 0.093 ± 0.019 V) as the innocuous test object for the medium-size category.

SPHERICAL TEST OBJECTS

Nonspherical test objects manifest a rotational dependence (see [fig. 7](#)) in their detectability that may affect the qualification of a WTMD to perform as required. That is, the rotation may cause the threat object to appear larger than it is and thus incorrectly qualify the WTMD to detect the smaller threat object. The replacement of a nonspherical test object by a spherical test object for establishing the detectability of a set of threat objects represented by that test object should be based on the orientation of the nonspherical test object that provides its least detectability. The spherical test object that is selected should be less detectable than the nonspherical object in its least-detectable orientation at all entry-point locations, as this will ensure a high likelihood of detecting the threat objects it is intended to represent, regardless of the orientation of the threat object. In this section, and for the purpose of illustration, only two examples of using a spherical test object in lieu of the traditional test object will be presented.

Large-Size Test Objects

The least-detectable large-sized ferromagnetic test object is the NIJ Standard 0601.02 steel handgun exemplar, fabricated using steel UNS G41400. [Figure 10](#) shows the $max_{obj,loc}$ for the NIJ Standard 0601.02 steel handgun exemplar (indicated as “steel handgun”) and solid steel (UNS G41300) spheres of varying diameters. This figure shows that the detectability of the 50-mm-diameter sphere is greater than that of the steel handgun exemplar, whereas the 40-mm-diameter sphere’s detectability is less than that of or nearly the same as (within 2 standard deviations) the steel knife exemplar for all entry-point locations. Therefore, if the WTMD can detect a 40-mm-diameter steel sphere, it will detect the steel handgun exemplar and all other more detectable test objects or threat items.

Small-Size Test Object

The least detectable of the typical small nonferromagnetic test objects is the 22-caliber round, often represented by the NIJ Standard 0601.02 22-caliber-round exemplar. [Figure 11](#) shows the $max_{obj,loc}$ for the NIJ Standard 0601.02 22-caliber-round exemplar and solid aluminum (UNS A96061) spheres of varying diameters. This figure shows that the detectability of the 9-mm-diameter sphere is greater than that of the 22-caliber-round exemplar, whereas the 8-mm-diameter sphere’s detectability is less than that of the 22-caliber-round exemplar for all entry-point

FIG. 10

$max_{obj,loc}$ for the test objects indicated. The steel handgun is made of solid steel (UNS G41400) and the spheres are solid steel (UNS G41300).

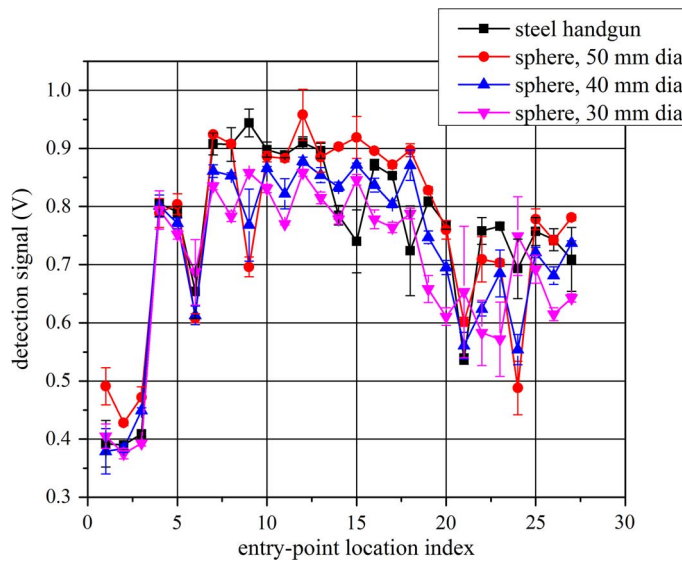
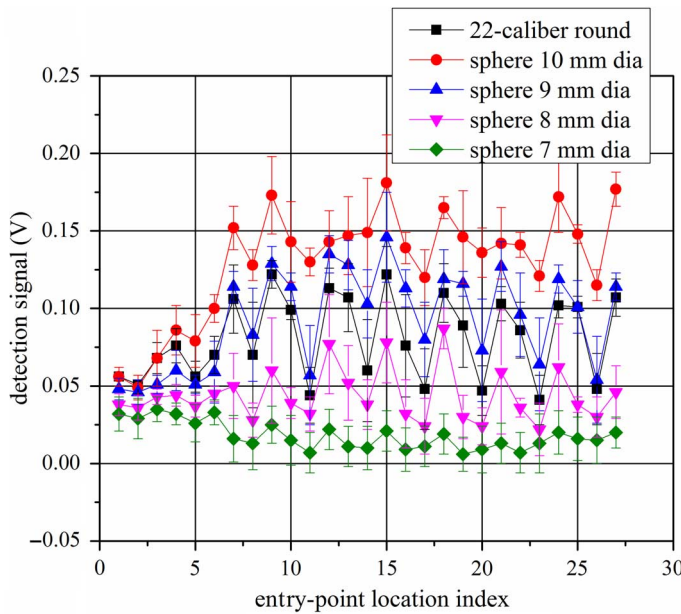


FIG. 11

$max_{obj,loc}$ for the test objects indicated. The spheres are made of solid aluminum (UNS A96061).



locations. Therefore, if the WTMD can detect an 8-mm-diameter aluminum sphere, it will detect a 22-caliber round and all other more detectable test objects or threat items.

Innocuous-Item Test Objects

The purpose of the innocuous object is to aid in adjusting the sensitivity of the WTMD so that it will not alarm on items deemed to not be a threat. One approach is to have a unique set of innocuous items (see the “Test Objects for p_{fa} ” section). Another approach is to have the innocuous item be one size smaller than the size classification

being tested, as described in the section “ p_{fa} (Innocuous) Test Objects.” However, from a baseline performance perspective, it is not necessary that the innocuous-item test object resembles an actual innocuous item encountered in practice. Consequently, the use of spheres is a reasonable approach for the design of the innocuous-item test objects, and it avoids the effects of rotation and orientation on its detectability and the measurement uncertainty associated with these effects.

Conclusions

Currently used and industry-accepted test objects were examined for use in evaluating the baseline technical performance of WTMDs. The test objects that represent threats and that should be used to test the detection performance of WTMDs should be the least detectable of a given size category to ensure that any threat-based test objects that are more detectable than the least-detectable threat-based test object would be discovered. It was determined that the test objects described in NIJ Standard 0601.02 typically are the least detectable for the given size category, of which there are three for the WTMD: large, medium, and small, each category comprising one test object each of ferromagnetic and nonferromagnetic metals, giving six test objects for evaluating WTMD threat object detection performance. In two of these cases, the test object described in the NIJ Standard 0601.02 had to be modified to be the least detectable. The effect of rotation about the major orientation axes was also examined and shown to cause a difference in detectability of up to 30 % between the most and least-detectable rotations. This effect led to the examination of spheres as potential candidates to test WTMD threat object detection performance. Spheres eliminate the effects of test object rotation on test object detectability. For two of the six categories of test objects, a sphere was identified to provide an option for the least-detectable test object. Lastly, the innocuous-item test objects, which are used to assess nuisance alarms, was also examined. The detection signature of the selected innocuous-item test object should ideally be the greatest for its size category but less than the least-detectable threat-test object of that category. Because of orientation effects, these two bounds may approach each other. Consequently, it is recommended that the least detectable of the next-size-smaller threat object category be used as the innocuous-item test object for the threat object detection category being tested. For example, the least-detectable small-sized threat-item test object may be used to test the nuisance alarm rate for the WTMD medium-sized threat detection setting. Spherical test objects may be also used for innocuous-item test objects.

References

1. D. M. Sheen, D. L. McMakin, and T. E. Hall, “Three-Dimensional Millimeter-Wave Imaging for Concealed Weapon Detection,” *IEEE Transactions on Microwave Theory and Techniques* 49, no. 9 (2001): 1581–1592, <https://doi.org/10.1109/22.942570>
2. S. F. Hallowell, “Screening People for Illicit Substances: A Survey of Current Portal Technology,” *Talanta* 54, no. 3 (2001): 447–458, [https://doi.org/10.1016/S0039-9140\(00\)00543-9](https://doi.org/10.1016/S0039-9140(00)00543-9)
3. B. Elias, *Airport Body Scanners: The Role of Advanced Imaging Technology in Airline Passenger Screening*, CRS Report for Congress R42750 (Washington, DC: Congressional Research Service, 2012).
4. D. Larson, N. Paulter, and N. Troje, “Walk-through Metal Detector Testing and the Need to Emulate Natural Body Motion,” *Journal of Testing and Evaluation* 47, no. 1 (2019): 627–639, <https://doi.org/10.1520/JTE20170342>
5. N. Paulter, “Test Methods to Rigorously, Reproducibly, and Accurately Measure the Detection Performance of Walk-through Metal Detectors,” *Journal of Testing and Evaluation* 48, no. 2 (2020): 1694–1711, <https://doi.org/10.1520/JTE20180220>
6. National Institute of Justice, *Walk-Through Metal Detectors for Use in Concealed Weapon and Contraband Detection*, NIJ Standard 0601.02 (Washington, DC: U.S. Department of Justice, 2003), <http://web.archive.org/web/20200319171123/https://www.ncjrs.gov/pdffiles1/nij/193510.pdf>
7. *Standard Practice for Evaluation of Metallic Weapons Detectors for Controlled Access Search and Screening*, ASTM F1468-04a(2018) (West Conshohocken, PA: ASTM International, approved June 1, 2018), <https://doi.org/10.1520/F1468-04AR18>
8. P. Gao, L. Collins, P. M. Graber, N. Geng, and L. Carin, “Classification of Landmine-Like Metal Targets Using Wideband Electromagnetic Induction,” *IEEE Transactions on Geoscience and Remote Sensing* 38, no. 3 (2000): 1352–1361, <https://doi.org/10.1109/36.843029>
9. I. J. Won, D. A. Keiswetter, and T. H. Bell, “Electromagnetic Induction Spectroscopy for Clearing Landmines,” *IEEE Transactions on Geoscience and Remote Sensing* 39, no. 4 (2001): 703–709, <https://doi.org/10.1109/36.917876>

10. W. R. Scott, "Broadband Array of Electromagnetic Induction Sensors for Detecting Buried Landmines," in *IGARSS 2008 - 2008 IEEE International Geoscience and Remote Sensing Symposium* (Piscataway, NJ: Institute of Electrical and Electronics Engineers), II-375–II-378, <https://doi.org/10.1109/IGARSS.2008.4779006>
11. T. H. Bell, B. J. Barrow, and J. T. Miller, "Subsurface Discrimination Using Electromagnetic Induction Sensors," *IEEE Transactions on Geoscience and Remote Sensing* 39, no. 6 (2001): 1286–1293, <https://doi.org/10.1109/36.927451>
12. J. T. Miller, T. H. Bell, J. Soukup, and D. Keiswetter, "Simple Phenomenological Models for Wideband Frequency-Domain Electromagnetic Induction," *IEEE Transactions on Geoscience and Remote Sensing* 39, no. 6 (2001): 1294–1298, <https://doi.org/10.1109/36.927452>
13. Y. Zhang, L. Collins, H. Yu, C. E. Baum, and L. Carin, "Sensing of Unexploded Ordinance with Magnetometer and Induction Data: Theory and Signal Processing," *IEEE Transactions on Geoscience and Remote Sensing* 41, no. 5 (2003): 1005–1015, <https://doi.org/10.1109/TGRS.2003.810922>
14. H. H. Nelson and J. R. McDonald, "Multisensor Towed Array Detection System for UXO Detection," *IEEE Transactions on Geoscience and Remote Sensing* 39, no. 6 (2001): 1139–1145, <https://doi.org/10.1109/36.927427>
15. C. Nelson, V. Chaudhary, J. Edman, and P. Kantor, "Walk-Through Metal Detectors for Stadium Security," in *2016 IEEE Symposium on Technologies for Homeland Security* (Piscataway, NJ: Institute of Electrical and Electronics Engineers), 1–6, <https://doi.org/10.1109/THS.2016.7568969>
16. C. Nelson, P. Kantor, B. Nakamura, B. Ricks, R. Whytlaw, D. Egan, A. Matlin, F. Roberts, M. Tobia, and M. Young, "Experimental Designs for Testing Metal Detectors at a Large Sports Stadium," in *2015 IEEE Symposium on Technologies for Homeland Security* (Piscataway, NJ: Institute of Electrical and Electronics Engineers), 1–7, <https://doi.org/10.1109/THS.2015.7225280>
17. J. Skorupski and P. Uchronski, "A Fuzzy Model for Evaluating Metal Detection Equipment at Airport Security Screening Checkpoints," *International Journal of Critical Infrastructure Protection* 16 (March 2017): 39–48, <https://doi.org/10.1016/j.ijcip.2016.11.001>
18. L. A. Marsh, C. Ktistis, A. Järvi, D. W. Armitage, and A. J. Peyton, "Three-Dimensional Object Location and Inversion of the Magnetic Polarizability Tensor at a Single Frequency Using a Walk-through Metal Detector," *Measurement Science and Technology* 24, no. 4 (2013): 045102, <https://doi.org/10.1088/0957-0233/24/4/045102>
19. P. D. Ledger and W. R. B. Lionheart, "Understanding the Magnetic Polarizability Tensor," *IEEE Transactions on Magnetics* 52, no. 5 (2016): 1–16, <https://doi.org/10.1109/TMAG.2015.2507169>
20. *Standard Performance Specifications and Test Methods for Hand-Worn Metal Detectors Used in Safety and Security*, ASTM F3020-19a (West Conshohocken, PA: ASTM International, approved August 1, 2019), <https://doi.org/10.1520/F3020-19A>
21. *Standard Performance Specifications and Test Methods for Hand-Held Metal Detectors Used in Safety and Security*, ASTM F3278-19a (West Conshohocken, PA: ASTM International, approved August 1, 2019), <https://doi.org/10.1520/F3278-19A>
22. N. G. Paulter Jr., D. R. Larson, and J. A. Ely, "Test Object for Accurate and Reproducible Measurement of the Detection Response of Hand-Worn and Hand-Held Metal Detectors," *Journal of Research of the National Institute of Standards and Technology* 121 (2016): 401–419, <https://doi.org/10.6028/jres.121.019>
23. N. G. Paulter, D. Larson, and J. Ely, "Handheld Metal Detector Characterization Using Spherical Test Objects," *Journal of Testing and Evaluation* 48, no. 2 (2020): 1262–1276, <https://doi.org/10.1520/JTE20170339>
24. N. G. Paulter Jr., D. R. Larson, and R. H. Palm Jr., *A Measurement System for Characterizing the Detection Performance of Metal Detectors: Design and Operation*, NISTIR 6530 (Gaithersburg, MD: National Institute of Standards and Technology, 2000), <https://doi.org/10.6028/NIST.IR.6530>